A *Streptococcus* aquaporin acts as peroxiporin for efflux of cellular hydrogen peroxide and alleviation of oxidative stress

Received for publication, November 27, 2018, and in revised form, January 27, 2019 Published, Papers in Press, January 31, 2019, DOI 10.1074/jbc.RA118.006877

Huichun Tong[‡§1], **Xinhui Wang**[‡§], **Yuzhu Dong**[‡§], **Qingqing Hu**[‡§], **Ziyi Zhao**[¶], **Yun Zhu**[¶], **Linxuan Dong**[‡], **Fan Bai**[¶], and **Xiuzhu Dong**[‡§2]

From the [‡]*State Key Laboratory of Microbial Resources, Institute of Microbiology, Chinese Academy of Sciences, No. 1 Beichen West Road, Chaoyang District, Beijing 100101, China,* [§]*University of Chinese Academy of Sciences, No. 19A Yuquan Road, Shijingshan District, Beijing 100049, China,* [¶]*Biomedical Pioneering Innovation Center (BIOPIC), School of Life Sciences, Peking University, No. 5 Yiheyuan Road, Haidian District, Beijing 100871, China*

Edited by Ursula Jakob

Aquaporins (AQPs) are transmembrane proteins widely distributed in various organisms, and they facilitate bidirectional diffusion of water and uncharged solutes. The catalase-negative bacterium *Streptococcus oligofermentans* produces the highest H_2O_2 levels reported to date, which has to be exported to avoid oxidative stress. Here, we report that a *S. oligofermentans* aquaporin functions as a peroxiporin facilitating bidirectional transmembrane H_2O_2 transport. Knockout of this aquaporin homolog, So-AqpA, reduced H_2O_2 export by ~50% and increased endogenous H_2O_2 retention, as indicated by the cellular H_2O_2 reporter HyPer. Heterologous expression of *So-aqpA* accelerated exogenous H_2O_2 influx into *Saccharomyces cerevisiae* and *Escherichia coli* cells, indicating that So-AqpA acts as an H_2O_2-transferring aquaporin. Alanine substitution revealed Phe-40 as a key residue for So-AqpA–mediated H_2O_2 transport. Northern blotting, qPCR, and luciferase reporter assays disclosed that H_2O_2 induces a >10-fold expression of *So-aqpA*. Super-resolution imaging showed that H_2O_2 treatment increases So-AqpA protein molecules per cell by 1.6- to 3-fold. Inactivation of two redox-regulatory transcriptional repressors, PerR and MntR, reduced H_2O_2-induced *So-aqpA* expression to 1.8- and 4-fold, respectively. Electrophoretic mobility shift assays determined that MntR, but not PerR, binds to the *So-aqpA* promoter, indicating that MntR directly regulates H_2O_2-induced *So-aqpA* expression. Importantly, *So-aqpA* deletion decreased oxic growth and intraspecies competition and diminished the competitive advantages of *S. oligofermentans* over the caries pathogen *Streptococcus mutans*. Of note, *So-aqpA* orthologs with the functionally important Phe-40 are present in all streptococci. Our work has uncovered an intrinsic, H_2O_2-inducible bacterial peroxiporin that has a key physiological role in H_2O_2 detoxification in *S. oligofermentans*.

Aquaporins (AQPs)[3] belong to the major intrinsic protein (MIP) family and are widely distributed in all the cellular organisms. They form channels across biological membranes and facilitate bidirectional diffusion of water and small uncharged solutes, such as glycerol and urea (1, 2). Since their first discovery in 1992 (1), numerous studies have demonstrated that human AQPs display important physiological functions and their dysfunctions cause many clinical disorders (3, 4). The plant AQPs are found to be involved in transpiration, root water uptake, seed desiccation, inhibition of self-pollination, and closure of leaf guard cells (5, 6). Phylogenetically, MIPs are clustered into two clades, the water-transporting AQPs and the glycerol-permeable aquaglyceroporins (GLPs) (7). Both clades of the aquaporins possess an Asn-Pro-Ala (NPA) signature motif and an aromatic/arginine (ar/R) substrate selectivity filter; and ar/R consists of one conserved arginine and three other amino acids that are conserved within each subfamily (8). Like many other membrane transporters, the activities of AQPs are subjected to regulation. The eukaryotic water-transporting aquaporins can be regulated by protein trafficking (9), and phosphorylation, pH, or divalent cations mediated gating (10, 11). Recently, it was reported that pH regulates the permeability of an aquaglyceroporin, AQP7, by altering protonation of the key amino acid residues (12).

Probably because of the similar electrochemical properties of H_2O and H_2O_2, some AQPs can transport H_2O_2 through the H_2O channel (6, 13). In recent years, a growing number of animal and plant aquaporin homologs have been verified to transport H_2O_2, which can promote development of some important physiological characteristics in eukaryotes (14–16). The human AQP3 and AQP8 facilitate H_2O_2 permeating across the cell membranes (17), which allows mitochondria-generated H_2O_2, a key molecule in the redox signaling network, to permeate into other cellular compartments and regulate physiological processes (6, 16–19). However, being an oxidant, the H_2O_2 level has to be strictly controlled to prevent cells from oxidative stress, which would subsequently cause disease and tumorigenesis (5).

This study was supported by the National Natural Science Foundation of China Grant No. 31370098. The authors declare that they have no conflicts of interest with the contents of this article.

This article contains Figs. S1–S3 and Table S1.

[1] To whom correspondence may be addressed. Tel.: 86-10-6480-7567; Fax: 86-10-6480-7429; E-mail: tonghuichun@im.ac.cn.

[2] To whom correspondence may be addressed. Tel.: 86-10-6480-7413; Fax: 86-10-6480-7429; E-mail: dongxz@im.ac.cn.

[3] The abbreviations used are: AQP, aquaporin; qPCR, quantitative PCR; MIP, major intrinsic protein; GLP, glycerol-permeable aquaglyceroporin; PALM, photoactivated localization microscopy; BHI, brain heart infusion; a.u., arbitrary units; ROI, region of interesting; cfu, colony-forming unit; ANOVA, analysis of variance.

Because of the limited studies on prokaryotic AQPs (2, 20, 21), their functions are largely unknown, such as whether they also function to facilitate H_2O_2 excretion and whether this action has physiological significance. Based on the rate of H_2O_2 flux, Seaver and Imlay (22) found that a H_2O_2 transmembrane concentration gradient exists in *Escherichia coli*. This suggests that H_2O_2 permeability across the cellular membrane is limited, and the bacterial aquaporins may also function in facilitating H_2O_2 diffusion. Streptococci, a type of facultative anaerobic bacteria that lack catalase, are known to produce and accumulate high concentrations of H_2O_2 in cultures, indicating they possess effective H_2O_2 excretion pathways. Streptococci carry genes that encode two clades of aquaporins, AQPs and GLPs. Interestingly, our previous microarray analysis found increased expression of the AQP genes in H_2O_2-treated *Streptococcus oligofermentans*, a bacterium so far known to produce and tolerate the highest levels of H_2O_2 (23), implying that the AQPs might play a role in H_2O_2 excretion.

In the present study, we investigated the roles of *S. oligofermentans* aquaporins in facilitating H_2O_2 efflux and the regulatory mechanisms. Through the integration of genetic, physiological, biochemical, and single-molecule imaging approaches, we identified a streptococcal peroxiporin, So-AqpA. By using an intracellular-specific H_2O_2 fluorescence reporter, HyPer, we demonstrated that So-AqpA, with Phe-40 as a key residue, facilitated the bidirectional permeation of H_2O_2 across the cellular membrane. Northern blotting and quantitative PCR, and photoactivated localization microscopy (PALM) super-resolution imaging determined that H_2O_2 induced the expression of *So-aqpA* gene at both transcriptional and translational levels. The two well-known redox transcriptional regulators PerR and MntR are involved in the H_2O_2-induced expression of *So-aqpA*. Deletion of the *So-aqpA* gene caused oxidative stress and reduced the intraspecies and interspecies competitive advantages of *S. oligofermentans*. This work reports for the first time the physiological roles of a bacterial peroxiporin, which could be a potential target for suppression of streptococci, especially the pathogenic species.

Results

The aquaporin homolog So-aqpA encodes an H_2O_2 facilitator

The *S. oligofermentans* genome carries three MIP family homologous genes: I872_01445 encodes an aquaporin, so was designated as *So-aqpA* and the encoded protein designated as So-AqpA; I872_09070 and I872_03455 encode glycerol uptake facilitator proteins and are designated as *So-aqpB* and *So-aqpC*, respectively, and the encoded proteins were designated as So-AqpB and So-AqpC. *So-aqpC* belongs to a three-gene operon for glycerol metabolism; thereby it was predicted to facilitate glycerol uptake. Phylogenetically, So-AqpA is related to the *E. coli* aquaporin Z (b0875), whereas the two aquaglyceroporins (So-AqpB and So-AqpC) are related to the *E. coli* aquaglyceroporin GlpF (b3927) and the human aquaporin AQP3 (360) (Fig. 1*A*). To determine whether these MIP family proteins function as H_2O_2 transporters in *S. oligofermentans*, *So-aqpA* and *So-aqpB* were deleted and the mutants were designated as Δ*aqpA* and Δ*aqpB*, respectively. Given that streptococci produce and accumulate endogenous H_2O_2 under oxic conditions, the two mutants and WT strain were cultured statically, and then the exponential phase cells were resuspended in fresh BHI medium. After incubated at 37 °C for 1 h, H_2O_2 concentrations in the cultures were measured as described in "Experimental procedures." 113 ± 16 μM H_2O_2 was determined in the WT strain culture, whereas 64 ± 9 μM and 110 ± 13 μM H_2O_2 were determined in the Δ*aqpA* and Δ*aqpB* cultures, respectively. Next these three strains, and the *So-aqpA* complemented strain (*aqpA*-com) were cultured under higher oxygen supplies in 10 ml BHI in a 100-ml triangle flask for higher endogenous H_2O_2 production. Then H_2O_2 contents in the cultures were measured. We found that while about half amount of H_2O_2 was produced by the Δ*aqpA*, similar H_2O_2 yields were measured in the *aqpA*-com, the WT, and Δ*aqpB* strains (Fig. 1*B*). This suggests that So-AqpA is a H_2O_2 facilitator, but So-AqpB is not.

To further validate that So-AqpA acts as a H_2O_2 facilitator, its gene was heterogeneously expressed in *Saccharomyces cerevisiae* by the vector pYES2 and in *E. coli* by the vector pIB166 (24). As shown in Fig. 1*C*, good growth of the *S. cerevisiae* INVSc1 strain carrying a vacant vector occurred on the galactose agar plates that contained H_2O_2 up to 2.5 mM, whereas the *So-aqpA*–expressing strain grew poorly at 2 mM and no growth was shown at 2.5 mM H_2O_2. Accordingly, H_2O_2 minimal inhibitory concentration value was determined to be 3 mM for the *So-aqpA*–expressing strain compared with 6 mM for the empty vector–expressing *S. cerevisiae*. In addition, a green fluorescence protein (sfGFP)–*So-aqpA* fusion was introduced into strain INVSc1, and the GFP fluorescence around the cytoplasmic membrane was observed under a confocal laser scanning microscope, confirming the expression of *So-aqpA* in *S. cerevisiae* (Fig. 1*C*). Subsequently, *So-aqpA* facilitated H_2O_2 permeation into *E. coli* cells was tested by monitoring the dynamics of exogenous H_2O_2 reduction based on the cytoplasmic catalase scavenging. The mid-exponential phase Luria broth (LB) cultures of *E. coli* DH5α expressing pIB166-*aqpA* and the vacant pIB166 were suspended in PBS, and by using 150 μM H_2O_2 as the initial concentration, the residual H_2O_2 amounts were measured over time. As shown in Fig. 1*D*, *So-aqpA* expression increased about 8% H_2O_2 uptake rate of *E. coli* until 4 min, and about 6% increase until 8 min. Using quantitative RT-PCR, the transcript copies of *So-aqpA* and 16S rRNA in *E. coli* were quantified as 369,564 ± 94,966/μg cDNA and 335,341 ± 81,442 × 10^4/μg cDNA, respectively, thus, *So-aqpA* transcription in *E. coli* was determined as 0.11 ± 0.01 copies/1000 16S rRNAs. Taken together, these experiments demonstrated that So-AqpA is an H_2O_2 facilitator.

So-AqpA facilitates H_2O_2 efflux and influx

To test the direct involvement of So-AqpA in efflux of the *S. oligofermentans* endogenous H_2O_2, a HyPer fluorescent protein was used as an intracellular H_2O_2 reporter. The HyPer protein was constructed by Belousov *et al.* (25) by inserting the fluorescent protein cpYFP into the regulatory domain of the *E. coli* H_2O_2-sensing protein OxyR. When H_2O_2 oxidizes Cys-199 and Cys-208 to form a disulfide bond, HyPer emits green fluorescence. The *S. oligofermentans* lactate dehydrogenase promoter-HyPer gene fusion was inserted into the streptococci–

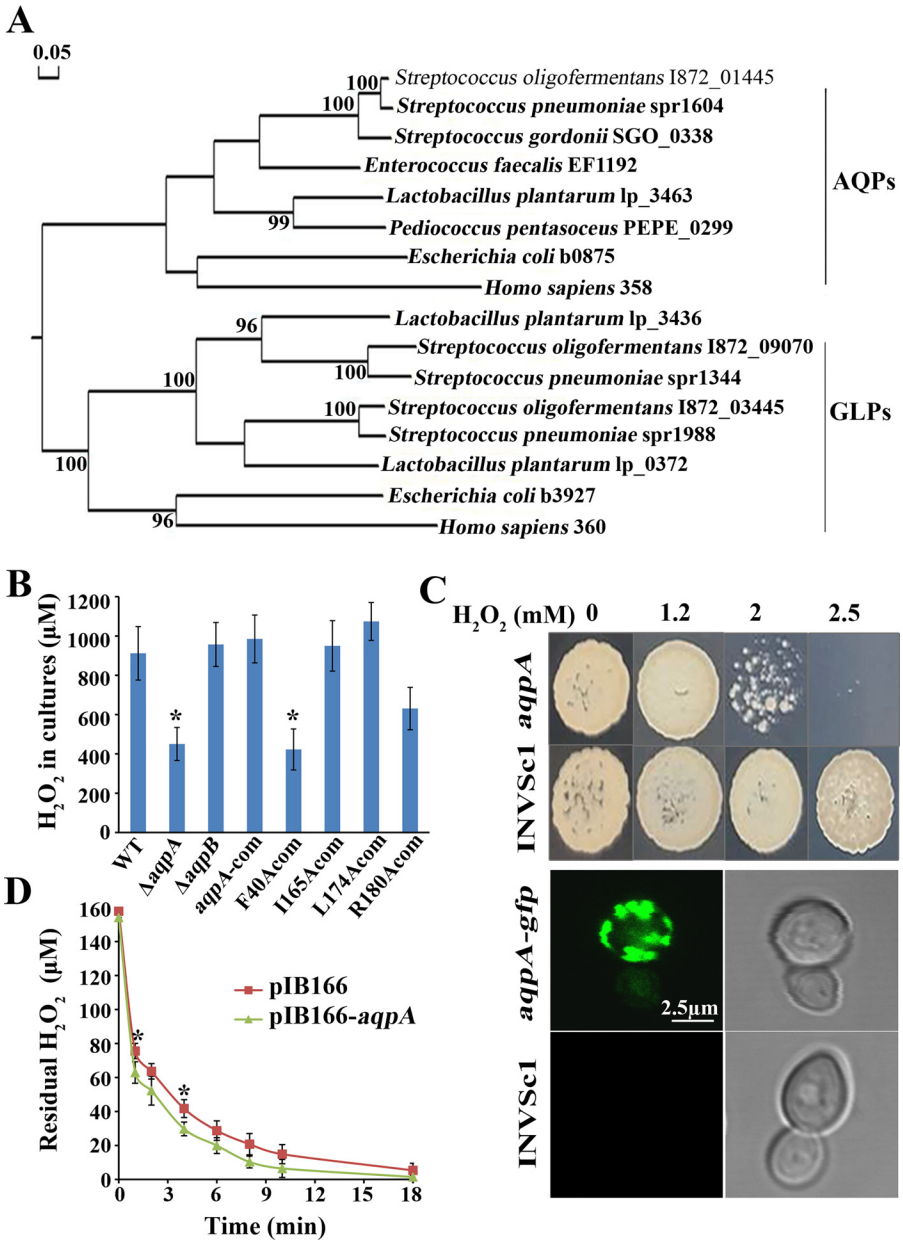

Figure 1. An aquaporin homolog *So-aqpA* encodes a H_2O_2 facilitator. *A*, phylogenetic analysis was performed for the *S. oligofermentans* aquaporin (I872_01445) and aquaglyceroporins (I872_09070 and I872_03455) with the homologs from representative lactic acid bacteria, *E. coli*, and humans. Protein sequences were retrieved from the NCBI protein database. The phylogenetic tree was constructed with DNAMAN using the neighbor-joining method and the bootstrap value was set as 1000. The *bar* of 0.05 represents the evolution distance. *B*, the WT strain, deletion mutants of *So-aqpA* and *So-aqpB*, and various point-mutated *So-aqpA* strains were cultured in 10-ml BHI broth in a 100-ml flask, and H_2O_2 yields in the stationary phase cultures were determined. The average ± S.D. from triplicate cultures of each strain are shown. *, data are statistically significant compared with those of the WT strain and the *So-aqpA* point mutation strains, as verified by one-way ANOVA followed by Tukey's post hoc test ($p < 0.05$). *C*, the *So-aqpA* gene either fused with the sfGFP gene or alone was integrated into the pYES2 plasmid and transformed into *S. cerevisiae* INVSc1. The INVSc1-*So-aqpA*, -*So-aqpA-gfp,* and -pYES2 strains were grown in SC-Ura-glucose for overnight, and then shifted to galactose to induce the *So-aqpA* gene expression. After a 6- to 8-h induction, 10 μl diluted INVSc1-*So-aqpA* and -pYES2 cultures (OD_{600} 0.01) were spotted on SC-Ura galactose agar plate which is supplemented with various concentrations of H_2O_2 (*upper panel*). The INVSc1-*So-aqpA-gfp* and -pYES2 cells were visualized under a confocal laser scanning microscope (Leica TCS SP8, Leica Microsystems) with excitation at 488 nm, and emission was collected from a range of 500 to 600 nm (*lower panel*). The representative GFP fluorescence (*left*) and differential interference contrast pictures (*right*) were shown. *D*, the *So-aqpA* gene was cloned into pIB166 and heterogeneously expressed in *E. coli*. Mid–exponential phase LB cultures (OD_{600} ~0.60) of the pIB166-*aqpA* and vacant pIB166 strains were collected by centrifugation and washed twice with PBS. Cells were then diluted into 10 ml PBS to OD_{600} 0.1, and a final concentration of 150 μM H_2O_2 was added. The residual H_2O_2 in PBS was then determined at the indicated time points. Average ± S.D. of triplicate experiments is shown. *, data were statistically significantly different from that of pIB166-*aqpA* strain at the corresponding time point (Student's *t* test, $p < 0.05$).

E. coli shuttle vector pDL278 (26) and introduced into *E. coli* DH5α cells. A similar peak of HyPer fluorescence, as reported previously (27), was observed in the *E. coli*–HyPer strain after 1-min treatment by 20 μM H_2O_2 (Fig. S1*A*). Following that, the pDL278-HyPer plasmid was introduced into the *S. oligofermentans* WT strain, Δ*aqpA* and the pyruvate oxidase deletion mutant (Δ*pox*) (28) to generate cellular H_2O_2 real-time reporter strains WT-HyPer, Δ*aqpA*-HyPer, and Δ*pox*-HyPer, respectively.

Next, So-AqpA-facilitated H_2O_2 export was examined in the three H_2O_2 real-time reporter strains that were cultured stati-

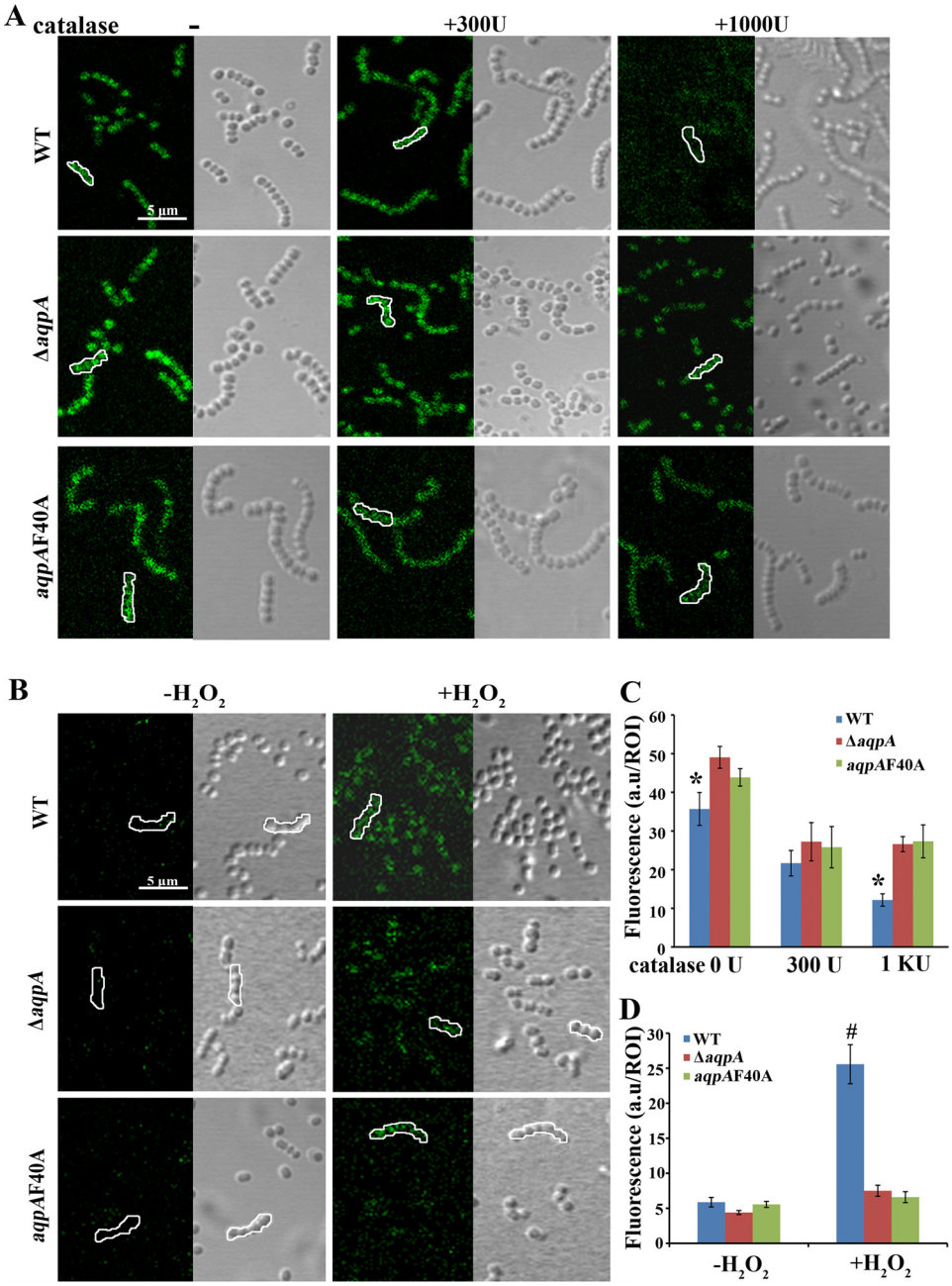

Figure 2. *S. oligofermentans* So-AqpA facilitates H_2O_2 transmembrane diffusion. *A*, the cellular H_2O_2 reporter HyPer fluorescence protein gene was introduced into all tested strains. The WT strain, *So-aqpA* deletion mutant (Δ*aqpA*), and its Phe-40 substitution mutant (*aqpA*F40A) were cultured statically in BHI broth containing 0 units (−), 300 units, and 1000 units catalase, respectively. The exponential phase cells were collected, washed, and resuspended in 100 μl PBS, and after a 30-min air exposure in dark, 40 μl cells were visualized under a confocal laser scanning microscope (Leica TCS SP8, Leica Microsystems) with excitation at 488 nm and emission collected from a range of 500 to 600 nm. *Bar*, 5 μm. *B*, mid–exponential phase anaerobically grown cells were resuspended in 100 μl PBS and pulsed by 0.5 mM H_2O_2. 40 μl of cells were sampled for visualization under a confocal laser scanning microscope before and 5 min after H_2O_2 pulsing. The results shown are representative of three independent experiments. *Left* and *right panels* in each picture show the cells with HyPer fluorescence and differential interference contrast, respectively. *Bar*, 5 μm. *C* and *D*, cell HyPer fluorescence intensity was measured using the Leica Application Suite Advanced Fluorescence software. At least five images were captured for each sample, and 25 ROI (framed) by each, including five cells in *panels A* (*C*) and *B* (*D*), were measured for calculation of the average fluorescence intensities. For images with too weak fluorescence to observe the cells, ROI in the corresponding differential interference contrast picture was framed and the fluorescence intensity was measured in the same ROI of the fluorescence image. Average fluorescence intensities were calculated and expressed as arbitrary unit (*a.u*) per ROI. * and #, data are statistically significantly different between the wild strain and the mutants as verified by one-way ANOVA analysis followed by Tukey's post hoc test ($p < 0.05$).

cally in BHI broth supplemented with 0 units, 300 units, and 1000 units catalase, respectively. Catalase was used to hydrolyze excreted H_2O_2 during growth so as to create an H_2O_2 gradient across cell membrane. The exponential phase cells were collected, and HyPer fluorescence was observed under a confocal laser scanning microscope. Fig. 2*A* showed significantly higher HyPer fluorescence intensity (~28 a.u. per region of interesting (ROI)) in 1000 units catalase-treated Δ*aqpA*-HyPer cells compared with the WT-HyPer strain (~12 a.u. per ROI), whereas only slightly higher intensities were observed in 0 units and 300 units catalase-treated mutant cells (Fig. 2*C*). No HyPer fluorescence was observed at all in the Δ*pox*-HyPer cells at the earlier

growth phase (Fig. S1*B*); this is consistent with the fact that the *pox* gene encoded pyruvate oxidase contributes to H_2O_2 production at the earlier growth phase of *S. oligofermentans* (28). This demonstrated that the *S. oligofermentans aqpA* gene encodes an H_2O_2 facilitator protein, and absence of the protein led to endogenous H_2O_2 retention. Although antibiotics can induce H_2O_2 production in bacteria, the observed HyPer fluorescence difference should be attributed to the studied genes, because all of the tested HyPer reporter strains were grown in BHI broth plus spectinomycin to maintain the shuttle plasmid.

To explore the role of So-AqpA in facilitating H_2O_2 influx, 2 ml mid–exponential phase cells of anaerobically grown WT-HyPer and Δ*aqpA*-HyPer cells were collected and resuspended in PBS. Cells were first exposed to air for 15 min and then pulsed with 0.5 mM H_2O_2. Fluorescence of the WT-HyPer cells was observed at 5 min post pulsing under a confocal laser scanning microscope. However, only weak fluorescence was observed in the Δ*aqpA* mutant (Fig. 2*B*), which was 5-fold lower than that in the WT strain (Fig. 2*D*). These results demonstrate that So-AqpA functions as a H_2O_2 facilitator for its bidirectional diffusion across the cellular membrane.

The key amino acid residues of So-AqpA for H_2O_2 permeation

To probe the key amino acids of So-AqpA that are involved in H_2O_2 transport, we first performed an amino acid sequence alignment with the phylogenetic orthologs from eukaryotic and prokaryotic species. As shown in Fig. 3*A*, So-AqpA possesses the two characteristic NPA motifs and the four conserved amino acid residues for AQP substrate binding (29). Homology modeling of the So-AqpA protein was performed by automatic selection of the *Archaeoglobus fulgidus* aquaporin (identity 44%) as a template via the SWISS-MODEL web service. Fig. 3*B* shows that So-AqpA is a tetramer with each monomer forming a barrel shape, and the conserved Phe-40, Ile-165, Leu-174, and Arg-180 are situated at the substrate-binding sites, the two NPA motifs meet at the central part of the channel (Fig. 3*C*). Next, alanine substitution was performed for the four substrate-binding residues, and each of the residue-substituted So-AqpA mutants was introduced into the Δ*aqpA* strain by shuttle vector pIB166. Using the same approach as described above, we determined that alanine substitution of Phe-40 (F40A) substantially and Arg-180 (R180A) moderately reduced H_2O_2 excretion, respectively (Fig. 1*B*). Mutation of the remaining two had no effect on excreted H_2O_2 content.

The effect of So-AqpA F40A mutation on H_2O_2 excretion was also tested using the HyPer fluorescence reporter. To accomplish this, F40A mutation was introduced into the chromosome at the *So-aqpA* locus to construct *aqpA*F40A strain, and then the HyPer fluorescence reporter was introduced into *aqpA*F40A strain to construct an *aqpA*F40A-HyPer strain. By comparing the HyPer fluorescence intensity with those of the WT-HyPer and Δ*aqpA*-HyPer strains, failure of H_2O_2 efflux and influx was observed for the *aqpA*F40A-HyPer strain. As shown in Fig. 2, either by suspending the cells in 1000 units catalase-contained fresh BHI or by pulsing with 0.5 mM H_2O_2, similar HyPer fluorescence intensities were found for the *aqpA*F40A and Δ*aqpA* strain. Collectively, these experimental evidences demonstrate that Phe-40 is a key residue for So-AqpA to facilitate H_2O_2 transport.

H_2O_2 induces transcription of the So-aqpA gene

To investigate the link between So-AqpA's function as a H_2O_2 facilitator and its role in detoxification for the bacterium, H_2O_2 induction of the *So-aqpA* expression was detected using Northern blotting and quantitative real-time PCR (qPCR) assays. A final concentration of 40 μM H_2O_2 was added into the mid–exponential phase cultures of *S. oligofermentans* that were grown anaerobically, and the same volumes of H_2O were added to the non-H_2O_2 treatment controls. By using a DNA fragment of the *So-aqpA* gene as probe (Table S1), Northern blotting detected an RNA of about 0.7 kb only in H_2O_2-treated cells, indicating that 40 μM H_2O_2 significantly induced *So-aqpA* transcription (Fig. 4*A*); consistently, the qPCR assay also determined a 10.5-fold elevated abundance of the *So-aqpA* mRNA in response to 40 μM H_2O_2 (Fig. 4*B*). To test whether the endogenous H_2O_2 affected *So-aqpA* expression, its transcription was compared in the statically cultured WT strain and a double-gene deletion mutant of *pox* and *lox*, which encode the two primary H_2O_2 production proteins, pyruvate and lactate oxidase (28). As expected, qPCR determined a 4.3-fold reduced expression of the *So-aqpA* gene in the *pox*/*lox* double mutant (Fig. 4*B*).

A luciferase reporter was then used to test the *So-aqpA* expression profile in response to endogenous H_2O_2 during growth. The *So-aqpA* gene promoter was fused to the *luc* gene on pFW5-*luc* (30), and luciferase activities were determined during growth of the statically or anaerobically cultured *S. oligofermentans*. Fig. 4*C* shows that under static growth condition, relatively higher expression of the *So-aqpA* gene occurred at the earlier exponential phase, corresponding to the peak expression periods of the *pox* gene and H_2O_2 production (28). Luciferase reporter determined 2.7- to 26.7-fold higher activities in the statically grown cells than those in the anaerobically grown cells during the entire growth period, consistent with qPCR assayed up-regulation of *So-aqpA* in the static culture (Fig. 4*B*). This demonstrated that when cells accumulated relative high H_2O_2, expression level of the *So-aqpA* gene would be enhanced to fulfill its task in excreting endogenous H_2O_2 and attenuating oxidative stress in *Streptococcus*.

Super-resolution PALM imaging reveals numerous So-AqpA protein molecules in H_2O_2-induced cell membrane

Subsequently, we investigated how many So-AqpA protein molecules are present in one bacterial cell so as to meet the requirement for efficient endogenous H_2O_2 efflux. To accomplish this, the state-of-the-art super-resolution imaging method of PALM (31) was employed to obtain high-resolution cell images. First, a chromosomal AqpA-mMaple3 fusion was constructed in which the *So-aqpA* gene was tagged with the monomeric photoactivatable fluorescent protein mMaple3 (32). To visualize the So-AqpA protein expression in different growth phases and also in response to H_2O_2, the AqpA-mMaple3 strain was cultured statically and anaerobically, respectively. Cells of the static culture were collected at its earlier and mid-exponential growth phases and suspended in PBS

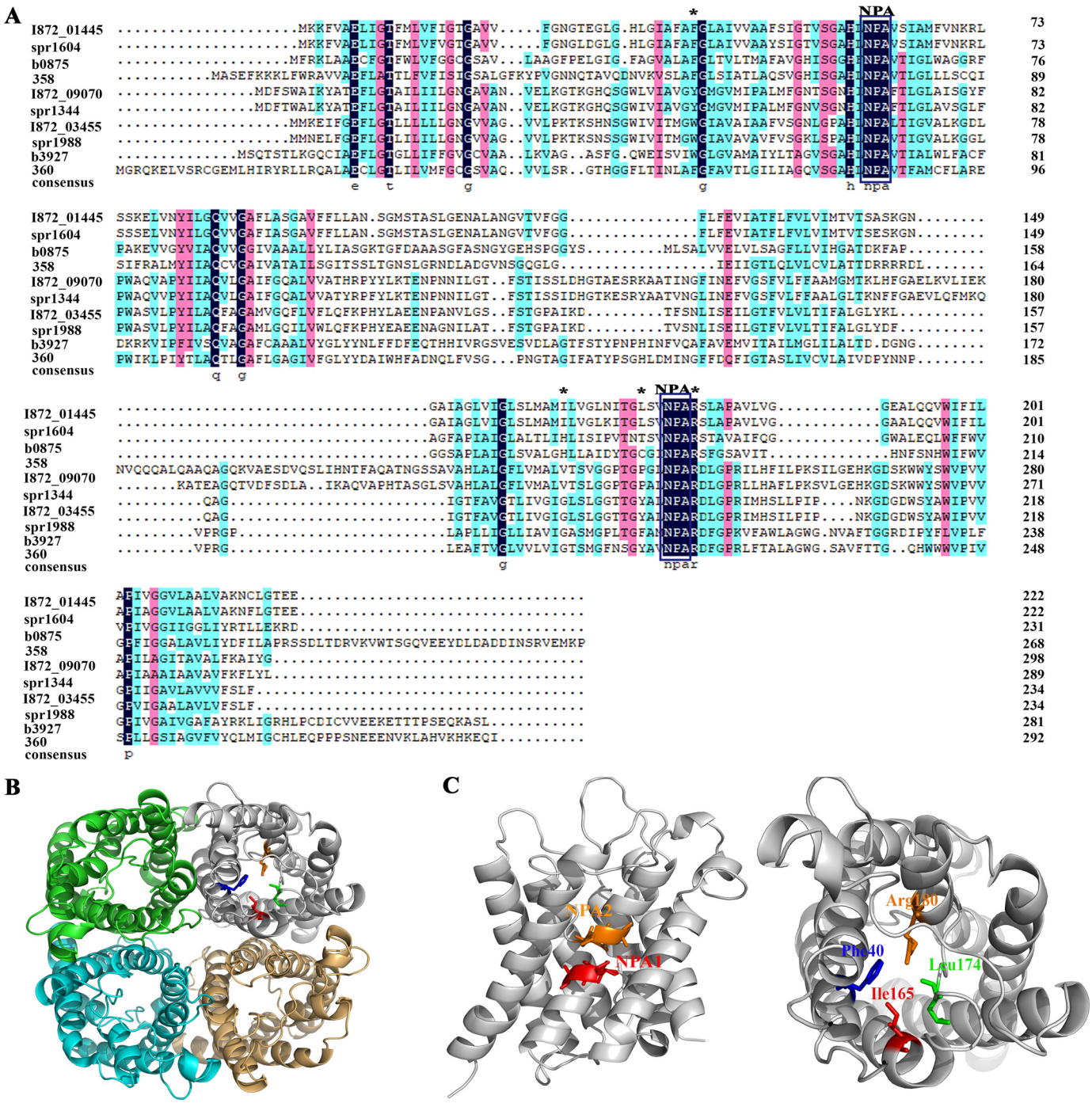

Figure 3. Structural analysis of the *S. oligofermentans* aquaporin protein So-AqpA. *A*, amino acid sequence alignment of the MIPs from *S. oligofermentans* (I872_01445, I872_09070, I872_03455), *S. pneumoniae* (spr1604, spr1344, spr1988), *E. coli* (b0875, b3927), and humans (358 and 360). The ar/R selective filter residues, FH(I)XR (X, small uncharged residues) in AQPs or WGFR in GLPs are labeled with asterisks, and the two NPA motifs are framed. *B* and *C*, structure modeling shows So-AqpA as a tetramer (*B*), the conserved ar/R selective filter residues Phe-40, Ile-165, Leu-174, and Arg-180 are situated at the substrate-binding sites, and the two NPA motifs meet at the central part of the channel (*C*).

buffer after washing. For the anaerobic culture, the mid-exponential phase cells were collected, and one aliquot was treated with 40 μM H_2O_2 for 20 min, whereas another was treated with the same volume of H_2O. Fig. 5*A* shows the representative PALM images of the So-AqpA-mMaple3 fusion fluorescent proteins on cell membrane, each image included a cell chain consisting of three or four single cells. The mMaple3 signals indicated abundant So-AqpA protein molecules distributed on the cytoplasmic membrane. By using the Insight3 software, the protein numbers were counted on 18 cells for each sample (33), and the calculated So-AqpA protein molecules were 131 ± 22 and 122 ± 17 per cell in the earlier and mid–exponential phase statically grown culture, respectively. However, only an average of 41 ± 9 So-AqpA molecules per cell were counted in the anaerobic culture; and the protein number was increased by 1.6-fold upon H_2O_2 treatment (Fig. 5*B*). The super-resolution imaging not only reveals that *S. oligofermentans* possesses numerous transmembrane peroxiporin molecules, but also validates H_2O_2 induc-

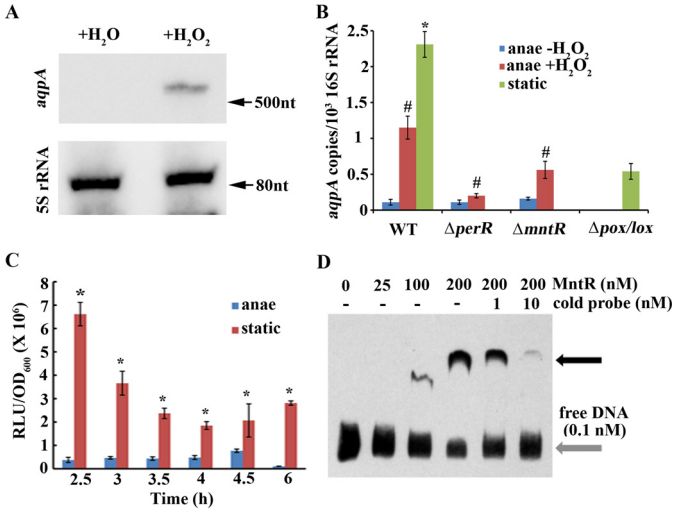

Figure 4. H_2O_2 induces the expression of the *So-aqpA* gene. *A*, anaerobically grown mid–expansion phase cells were collected and divided into two aliquots. One aliquot was treated with 40 μM H_2O_2 (+H_2O_2) for 20 min and the other with the same volume of H_2O (+H_2O) used as a control. Total RNA was extracted from both aliquots, and Northern blotting was performed using a biotin-labeled *So-aqpA* DNA fragment (Table S1) as the probe. 5S rRNA was used as an internal control (details are described in "Experimental procedures"). *B*, the tested strains were cultured and treated with 40 μM H_2O_2 as described in *A*. Quantitative RT-PCR was performed to quantify the transcript copies of the *So-aqpA* gene in anaerobically grown (*anae* $-H_2O_2$) and 40 μM H_2O_2-pulsed (*anae* $+H_2O_2$) wild strain (WT), deletion mutants of *perR* (Δ*perR*) and *mntR* (Δ*mntR*), and statically grown (*static*) wild strain and *pox* and *lox* double deletion mutant (Δ*pox/lox*) (details are described in "Experimental procedures"). Triplicate measurements were performed for three batches of cultures, and the averages ± S.D. are shown. * and #, data are statistically significantly different in comparison between statically grown WT strain and Δ*pox/lox* mutant (Student's *t* test, $p < 0.05$) and H_2O_2 induction on anaerobically grown WT strain and mutants as verified by one-way ANOVA analysis followed by Tukey's post hoc test ($p < 0.05$), respectively. *C*, a luciferase reporter strain, P*aqpA-luc*, in which the *So-aqpA* promoter was fused to the luciferase gene, was grown in BHI broth anaerobically or statically. At the indicated time points during growth, 100 μl cultures were collected in 1.5-ml Eppendorf tubes, and after 5 min exposure to air at room temperature, the luciferase activities (*RLU*, relative light units) were measured as described in "Experimental procedures." OD_{600} was measured in parallel. Triplicate measurements were performed for three batches of cultures, and the averages ± S.D. are shown. *, data are statistically significant compared with those of anaerobically grown WT strain as verified by Student's *t* test ($p < 0.05$). *D*, a DNA fragment of the *So-aqpA* promoter was PCR amplified with 5′-end biotin-labeled primers (Table S1). 0.1 nM biotin-labeled DNA was mixed with various concentrations of MntR protein in the EMSA-binding mixture and run in a native PAGE gel. *Black arrow* indicates the protein-DNA complex. Addition of increasing nonlabeled DNA (*cold probe*) decreased the protein-DNA complex.

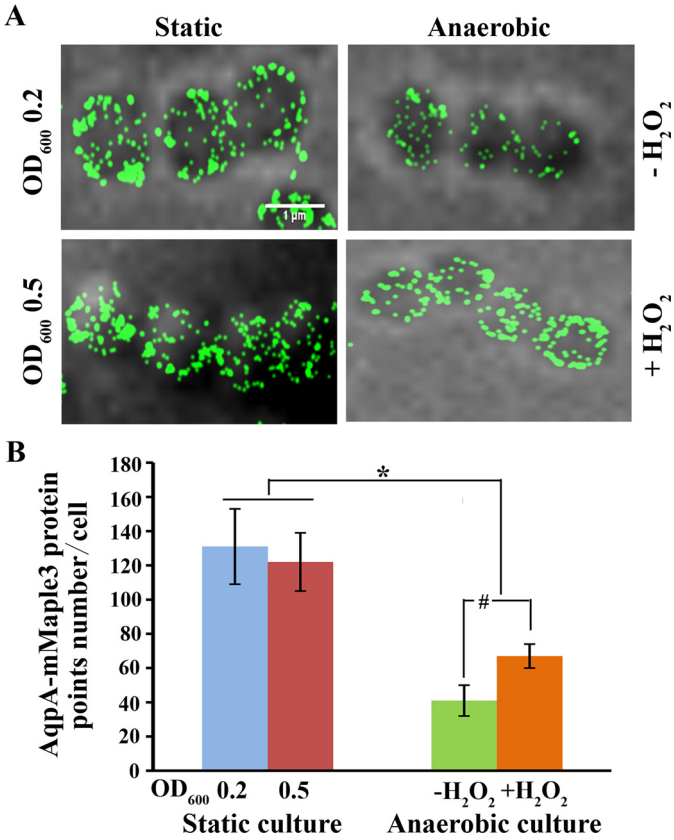

Figure 5. Representative PALM images show H_2O_2-induced So-AqpA protein abundance. *S. oligofermentans* with a chromosomal AqpA-mMaple3 fusion was grown statically and anaerobically, respectively. The static cultures were collected at the earlier (OD_{600} ~0.2) and mid-exponential phase (OD_{600} ~0.5) and suspended in PBS after washing. The anaerobically cultured cells were collected at mid-exponential phase (OD_{600} ~0.5), by one aliquot treated with 40 μM H_2O_2 for 20 min before observation. *A*, cells were observed using PALM super-resolution imaging. *B*, for each sample, at least three images were captured, and 18 representative cells were selected for quantification of So-AqpA protein by using the custom-written MATLAB scripts. # and *, data are statistically significant, as verified by one-way ANOVA analysis followed by Tukey's post hoc test ($p < 0.05$), compared with that of anaerobically grown WT strain without H_2O_2 treatment, and between the static and anaerobic cultures, respectively.

tion of the So-*aqpA* gene expression. This robust approach is particularly powerful for detection of the membrane proteins that are difficult to be assayed by Western blotting.

MntR and PerR are involved in regulation of H_2O_2-induced expression of So-aqpA

To further explore the regulatory mechanisms that mediate H_2O_2 induction of the *So-aqpA* expression, we tested the possible involvement of two known redox regulatory repressors, the metalloregulator MntR (34) and the peroxide-responsive repressor PerR (35). Our unpublished transcriptomic data[4] also showed that by deletion of either *mntR* or *perR*, H_2O_2-induced *So-aqpA* expression appeared to be attenuated. Δ*mntR* and Δ*perR* strains were then cultured anaerobically, and one aliquot of the mid–exponential phase cell was treated with 40 μM H_2O_2 while another was treated with the same volume of H_2O. After incubation at 37 °C for 20 min, the *So-aqpA* transcript copies were quantified by qPCR. As shown in Fig. 4*B* comparing with the >10-fold induction of *So-aqpA* expression by H_2O_2, the induction was reduced to 4- and 1.8-fold in the *mntR* and *perR* deletion mutants, respectively. This confirmed a regulatory involvement of the two regulators in H_2O_2-induced *So-aqpA* transcription.

To determine whether the two regulatory repressors directly regulate the expression of *So-aqpA*, EMSA was performed to detect the associations of overexpressed MntR and PerR proteins with 5′-biotin–labeled *So-aqpA* promoter fragment. As shown in Fig. 4*D*, a protein-DNA complex appeared at a 1000:1 ratio of MntR to DNA, a comparable affinity to its regulated manganese transporting protein *mntABC* promoter in a parallel experiment (Fig. S2); this complex disappeared with addition of the competing nonlabeled cold probe. This indicates that MntR may directly regulate the expression of *So-aqpA*. Additionally, a putative MntR-binding sequence (TATTAT$_{AACCTA}$ AAAATT, subscript letters indicate non-conserved bases) was

[4] H. Tong, X. Wang, Y. Dong, Q. Hu, Z. Zhao, Y. Zhu, L. Dong, F. Bai, X. Dong, unpublished data.

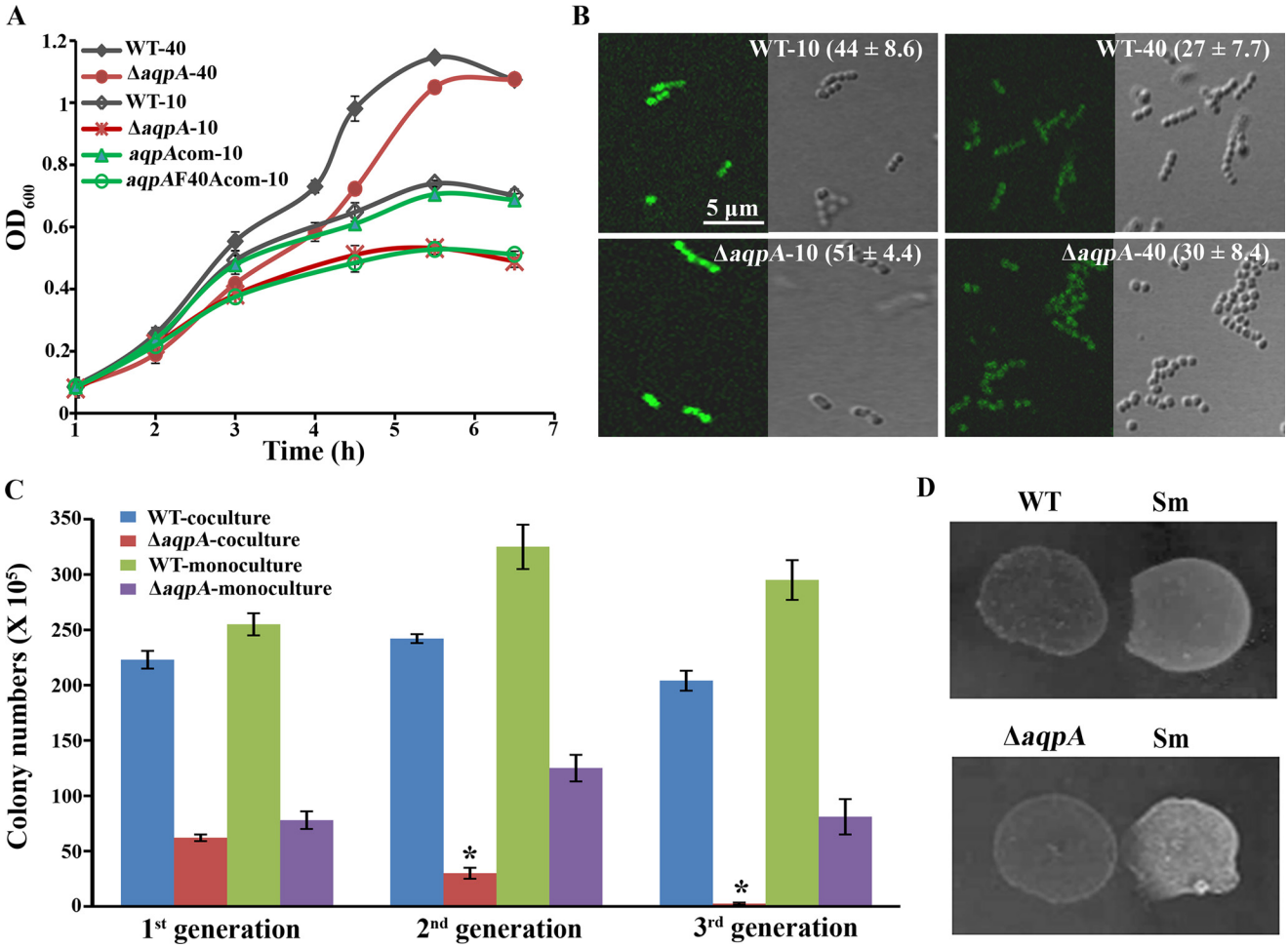

Figure 6. So-AqpA promotes the oxic growth and intraspecies and interspecies competitive advantage of *S. oligofermentans*. *A*, growth profiles were determined for the WT strain, *So-aqpA* mutant (Δ*aqpA*), *So-aqpA* complemented (*aqpA*com), and the Phe-40 substitution complemented (*aqpA*F40Acom) strains that were statically cultured in 10 ml or 40 ml BHI broth. Overnight BHI cultures of the tested strains were 1:30 inoculated into fresh BHI medium and incubated at 37 °C, and OD_{600} was measured at the indicated time. The results are expressed as averages ± S.D. of three independent experiments. Suffix numbers after strain names indicate the culture volumes. *B*, exponential growing cells from the cultures above were collected, and HyPer fluorescence was observed and measured using the same procedure as described in Fig. 2. Representative images of three independent experiments are shown and fluorescence intensity a.u. per ROI is shown inside the parentheses in each image. *Bar*, 5 μm. *C*, competition between the wild strain and *So-aqpA* mutant was determined for three successive subcultured generations under high oxygen content. The same amounts of the two strains were co-inoculated or mono-inoculated into 10 ml BHI broth contained in a 100-ml flask, and the co-culture and mono-culture were subcultured for three successive generations. Colony-forming units (cfu) of each culture in each generation were counted on BHI agar plate; BHI plate containing 1 mg/ml kanamycin was used to count cfu of the Δ*aqpA* mutant in co-cultures. The results are averages ± S.D. of three independent experiments. *, significantly different from the *So-aqpA* deletion mutant in the first generation of co-culture as verified by one-way ANOVA analysis followed by Tukey's post hoc test ($p < 0.05$). *D*, growth suppression of *S. mutans* (*Sm*) by the *S. oligofermentans* WT strain and *So-aqpA* mutant (Δ*aqpA*) was tested on TPYG plate (0.5% tryptone, 0.5% peptone, 1% yeast, 1% glucose, 4% salt solution) (23). Overnight cultures of the tested strains were collected and adjusted to the same OD_{600}. 10 μl of each strain were spotted side-by-side on the plates and incubated at 37 °C in the candle jar for 24 h. The experiments were repeated three times, and one representative experiment is shown.

found at the *So-aqpA* promoter region, and this is consistent with a ~1.5-fold enhanced expression of *So-aqpA* detected in the *mntR* deletion mutant (Fig. 4*B*). We previously demonstrated that MntR is inactivated by H_2O_2 via cysteine oxidation (34), which may explain MntR-dependent H_2O_2 induction of the *So-aqpA* expression. However, direct association of PerR with *So-aqpA* promoter was not found (data not shown), and the regulatory mechanisms of PerR on *So-aqpA* expression need to be further explored.

So-AqpA–based H_2O_2 export alleviates oxidative stress and provides S. oligofermentans with both intraspecies and interspecies competitive advantages

Because the WT strain produced significantly higher H_2O_2 (912 ± 136 μM) in 10 ml than that (255 ± 108 μM) in 40 ml BHI broth, to investigate the physiological significance of So-AqpA, the *So-aqpA* mutants and WT strain were statically grown in 10 ml or 40 ml medium in a 100-ml flask to create relatively high and low oxygen contents, respectively. As expected, no large growth difference was observed for the Δ*aqpA* and WT strains in 40 ml culture. However, in 10 ml cultures, severely retarded growth was found for the Δ*aqpA*- and F40A-complemented strains, but little inhibition was found for the WT and *aqpA*-complemented strain *aqpA*-com (Fig. 6*A*). Growth inhibition was not found for the *aqpA*-L174Acom, *aqpA*-I165Acom, and *aqpA*-R180Acom strains (Fig. S3).

To link growth inhibition with endogenous H_2O_2, cellular H_2O_2 levels were monitored using HyPer reporter. The mid–exponential phase cells of the WT-HyPer and Δ*aqpA*-HyPer strains were examined under a confocal microscope. As shown

in Fig. 6*B*, in the cells from either 10 ml or 40 ml culture, higher HyPer fluorescence intensities were always observed in Δ*aqpA*-HyPer compared with the WT-HyPer strain, whereas for each strain, higher HyPer fluorescence intensity was always detected in 10 ml compared with 40 ml cultures. The growth and cellular H_2O_2 measurements indicated that the aquaporin protein plays a significant role in protecting the bacterium from oxidative stress that is imposed by its own H_2O_2 production.

To examine the survivability of the Δ*aqpA* mutant among its parental WT strain, we co-cultured the two under higher and lower O_2 contents, respectively, and monocultures of the two strains were included as controls. By inoculating the same cell amounts of Δ*aqpA* and the WT strain into 40 ml and 10 ml BHI broth contained in a 100-ml flask, respectively, and until the stationary phase, the co-cultures and monocultures in 10-fold serial dilutions were plated on BHI agar plate with or without 1 mg/ml kanamycin. Significantly lower cell numbers were counted for the *aqpA* mutant ($62 \pm 3 \times 10^5$ cells/ml) in the 10 ml co-culture compared with the WT strain ($22 \pm 8 \times 10^6$ cells/ml). No significant difference was found between the Δ*aqpA* ($60 \pm 12 \times 10^6$ cells/ml) and WT strain ($65 \pm 15 \times 10^6$ cells/ml) in the 40 ml BHI co-culture. Furthermore, upon three consecutive subcultures in 10 ml BHI, the percentage of the *So-aqpA* mutant gradually decreased from 21.7 to 1.2% in the first and third subculture of the co-culture (Fig. 6*C*), whereas cell numbers in the monospecies culture remained unchanged during subculturing. This further emphasizes the physiological significance of the aquaporin, which endows the bacterial cells with a selective advantage in intraspecies competition.

Previously, we found that *S. oligofermentans* overcompeted the caries-pathogen *Streptococcus mutans* using excreted H_2O_2, which is produced from the ample lactate generated by *S. mutans* so establishes a counterattack strategy (23). To determine the contribution of So-AqpA to this interspecies competition, the WT strain and Δ*aqpA* mutant were respectively spotted adjacent to *S. mutans* on TPYG plates. Fig. 6*D* shows that the Δ*aqpA* mutant grew poorer and only slightly suppressed *S. mutans* compared with the WT strain. To further quantify the inhibition of WT and Δ*aqpA* strain against *S. mutans*, the two strains were co-incubated with *S. mutans* as a mix-species culture, by including *S. mutans* single-species culture as control. After 24 h incubation, the cfu of *S. mutans* was counted based on its different colony appearance from that of *S. oligofermentans* (23). Compared with the cell number ($18 \pm 2 \times 10^7$ cells/ml) in monoculture, only 45% of live *S. mutans* ($81 \pm 11 \times 10^6$ cells/ml) was detected in the co-culture with *S. oligofermentans* WT strain, whereas the live cells ($145 \pm 13 \times 10^6$ cells/ml) were about 80% in the co-culture with Δ*aqpA*, thus the H_2O_2 excreted through So-AqpA can enhance about 35% inhibition effect of *S. oligofermentans*.

Discussion

In recent years, the physiological importance of aquaporin-facilitated transmembrane diffusion of H_2O_2, particularly in redox signaling, has been acknowledged in animals and plants (14–16). Yet, such information about the prokaryotic AQPs is almost missing. In this study, by using the ample H_2O_2-producing bacterium *S. oligofermentans* as a model, we demonstrated that a bacterial aquaporin, So-AqpA, functions to facilitate H_2O_2 transmembrane diffusion. The function not only detoxifies the endogenous H_2O_2 but also promotes the bacterium's intraspecies and interspecies competitive abilities. Notably, H_2O_2 significantly induces *So-aqpA* expression at both the mRNA and protein levels, and two redox transcriptional regulators, PerR and MntR, are involved in the H_2O_2 induction. Therefore, So-AqpA is most likely an intrinsic peroxiporin as named by Henzler and Steudle (36) and is the first reported bacterial AQP with physiological importance.

H_2O_2, as a by-product, is generated in all metabolic pathways with the involvement of oxygen, but this oxidant molecule is scavenged rapidly by catalase in aerobic organisms (22, 37, 38). However, in the catalase-negative lactic acid bacteria like lactobacilli and streptococci, H_2O_2 efflux is an effective approach for detoxification. Although these bacteria carry genes encoding both AQPs and GLPs, so far only one *in vitro* study indicates that three GLPs from *Lactobacillus plantarum* promote H_2O_2 sensitivity when they are heterogeneously expressed in yeast (21). Whether these GLPs act as H_2O_2 facilitators and their physiological importance in bacteria remain unknown. The present study demonstrated a water-facilitator type of AQP in an ample H_2O_2-producing streptococcus acting as a H_2O_2 facilitator and contributing to H_2O_2 detoxification. However, inactivation of the gene did not improve streptococcus hypertonic growth (data not shown), thus suggesting that So-AqpA is not primarily a water facilitator.

Remarkably, H_2O_2 induces the expression of *So-aqpA*, so indicating that it is an intrinsic peroxiporin (Figs. 4 and 5). Two transcriptional regulators, PerR and MntR, which are specifically involved in regulation of the cellular redox state, are involved in the H_2O_2 induction, and MntR is determined to be a direct regulator. It is also found that H_2O_2 induces a human water facilitator AQP, aquaporin-4; however, the oxidant appears not to directly induce the AQP synthesis but through H_2O_2-promoted phosphorylation of Cav1, which can indirectly modulate AQP4 subcellular distribution (39). In contrast, H_2O_2 induction of the *So-aqpA* expression appears to be at the transcriptional level and is mediated by the global H_2O_2-responsive regulators. Thus, H_2O_2-induced So-AqpA synthesis could be a strategy used by the catalase-lacking streptococci for dealing with the endogenous H_2O_2; when at higher levels, H_2O_2 can be speedily exported for detoxification with the assistance of large amounts of So-AqpA. Noticeably, a relatively lower H_2O_2 induction was found on synthesis of So-AqpA protein than the transcription of the gene (Figs. 4 and 5). This discrepancy could be because in general the cellular proteins have longer life spans than mRNAs, so larger alteration could be detected for transcript abundance when bacteria encounter changed environments. In addition, posttranscriptional or posttranslational regulation could occur for bacterial AQPs gene expression, similar as reported for the eukaryotic AQPs (9, 10, 11).

The substrate selectivity of AQPs is based on the proper substrate size and formation of energetically favorable hydrogen bonds between substrates and AQP amino acid residues in the substrate path (8, 40). Because water and H_2O_2 molecules possess similar physicochemical properties (41), it is predicted that the water-permeable AQPs also facilitate H_2O_2 diffusion. This

prediction is supported by some families of AQPs, such as the human AQP8 and AQP1, that are primarily water facilitators but also function in H_2O_2 permeation through cell membranes (42). In addition, the two molecules appear to pass through the same substrate channel, as transports of them are inhibited by the same amino acid mutations in eukaryotic AQPs (14). However, we cannot conclude that all AQPs transport H_2O_2, as the plant AQPs AtPIP2;3, AtPIP2;6, and AtPIP2;8 do not transport H_2O_2. Similarly, *E. coli* aqpZ (b0875) also does not transport H_2O_2 (20, 43, 44). So-AqpA may therefore represent a distinct type of AQP that acts primarily as a H_2O_2 facilitator, and its homologs are present in all the *Streptococcus* spp. and other catalase-negative bacteria like *Enterococcus* and *Lactococcus*. Such type of AQPs may also occur in plants, as expression of the *Solanaceae* XIP genes in yeast induce a high sensitivity to exogenous H_2O_2, even though they have no significant water-transport ability (45). Therefore, the distinct characteristics of the H_2O_2 facilitators need to be investigated but not limited to comparative analyses of the protein sequences.

Consistent with the majority of AQPs, So-AqpA is a six-transmembrane protein and possesses the conserved Asn-Pro-Ala motif which constitutes the substrate channel. Similar with most water-transporting AQPs, So-AqpA uses Phe-40 as one of the residues in the ar/R-selective filter, which was demonstrated to be the key residue for So-AqpA–mediated H_2O_2 transport. Differently, So-AqpA protein has no cysteine residue, which is present in almost all the eukaryotic AQPs (29, 46). This unique feature of the streptococcal aquaporins implies that it could be serve as a potential drug target for controlling infection of the pathogenic streptococci.

Collectively, this work reports a bacterial aquaporin that functions as a dedicated H_2O_2 facilitator (peroxiporin) and has important physiological roles for streptococci by detoxifying the endogenous H_2O_2 and endowing it intraspecies and interspecies competitive advantages.

Experimental procedures

Bacterial strains and culture conditions

S. oligofermentans AS 1.3089 (47) and its derivative strains (Table S1) were grown in brain heart infusion (BHI) broth (BD Difco, Franklin Lakes, NJ) statically or anaerobically under 100% N_2. Spectinomycin (1 mg ml^{-1}) or kanamycin (1 mg ml^{-1}) was used to select transformants.

Construction of genetic strains

All primers used in this study are listed in Table S1. *So-aqpA* and *So-aqpB* deletion strains were constructed using the PCR ligation method (48). The H_2O_2 reporter HyPer gene was amplified from the pHyPer-N1 plasmid, which was kindly provided by Prof. Jiangyun Wang at the Institute of Biophysics, Chinese Academy of Sciences, and fused to the *S. oligofermentans* lactate dehydrogenase gene (*ldh*) promoter by overlapping PCR; meanwhile, the *So-aqpA* promoter and coding gene were PCR amplified. The purified PCR products were integrated into the compatible sites of pIB166 or pDL278 plasmids, and the correct recombinant plasmids pDL278-HyPer or pIB166-*aqpA* were transformed into the WT strain or Δ*aqpA* mutant to produce HyPer or *So-aqpA* ectopically expressed strains. So-AqpA F40A, I165A, L174A, or R180A mutations were introduced into the pIB166-*aqpA* plasmid using a site-directed gene mutagenesis kit (Beyotime Biotechnology Co., Shanghai, China), and the correct constructs were transformed into the Δ*aqpA* mutant. The PCR-amplified monomeric gene sequence of the photoactivatable fluorescent protein mMaple3, which was kindly provided by Xiaowei Zhuang (Harvard University), was 3′ fused to the *So-aqpA* gene by overlapping PCR. Meanwhile, the F40A mutated *So-aqpA* gene was PCR amplified from the pIB166-*aqpA*F40A plasmid, and the purified PCR products were integrated into the *S. oligofermentans* WT genomic DNA via double crossover homologous recombination using kanamycin, amplified from plasmid pALH124 (49), as a selective marker to obtain *aqpA*F40A and *aqpA*-mMaple3 strains. pDL278-HyPer was transformed into the *aqpA*F40A strain to obtain *aqpA*F40A-HyPer.

Detection of intracellular hydrogen peroxide by HyPer imaging

Mid-exponential phase HyPer reporter cells were pelleted, washed with PBS twice, and resuspended in 100 μl of PBS in a 1.5 ml Eppendorf tube. After exposure to air for 30 min in the dark at room temperature, 40 μl of cells were placed on a glass slide (25 × 75 mm, 1- to 1.2-mm thick), covered with a coverslip (14 × 14 mm, 0.17-mm thick), and then visualized under a confocal laser scanning microscope (Leica TCS SP8, Leica Microsystems, Buffalo Grove, IL). Excitation was provided at 488 nm, with emission collected from a range of 500 to 600 nm. The gray values of 25 ROI by each containing five cells from each sample were measured using Leica Application Suite (LAS) Advanced Fluorescence software.

PALM imaging

The *aqpA*-mMaple3 strain was cultured statically and anaerobically. Cells of the static culture were collected at the indicated time by centrifugation, washed twice, and suspended in PBS. The anaerobic cultured cells were collected when OD_{600} reached ~0.5. One aliquot was treated with 40 μM H_2O_2 for 20 min and another aliquot was treated with the same volume of H_2O and used as a control. After PBS washing twice, cells were resuspended in PBS. All cells were exposed to air for 30 min in the dark at room temperature, then the cells were fixed with 4% paraformaldehyde for 15 min at room temperature, washed three times with PBS, and observed using PALM imaging. PALM imaging was performed using a Nikon TiE inverted microscope equipped with a 100 × oil-immersion objective (Nikon, PLAN APO, 1.49 NA) and an EMCCD camera (Andor-897). A 405-nm laser (Coherent, 100 milliwatt), 488-nm laser (Coherent, 100 milliwatt), and 561-nm laser (Coherent, 50 milliwatt) were used to either photoconvert or excite the fluorophores. AqpA-mMaple3 was activated with a continuous 405-nm laser, which was slowly increased for optimal photoconversion rates and excited with a constant 561-nm laser (~2 kilowatts/cm^2). 100 nm Tetraspeck beads (Invitrogen) were used to calibrate for stage drift during data acquisition. Construction of super-resolution images was performed using Insight3 software, kindly provided by Dr. Bo Huang (University of California San Francisco). PALM data analysis such as drift

correction and image rendering was carried out using custom-written MATLAB scripts.

Determination of the excreted hydrogen peroxide in culture

Hydrogen peroxide (H_2O_2) in culture suspension was quantified as described previously (35). Briefly, 650 μl of culture supernatant was added to 600 μl of solution containing 2.5 mM 4-amino-antipyrine (4-amino-2,3-dimethyl-1-phenyl-3-pyrazolin-5-one; Sigma) and 0.17 M phenol. The reaction proceeded for 4 min at room temperature; horseradish peroxidase (Sigma) was then added to a final concentration of 50 milliunits/ml in 0.2 M potassium phosphate buffer (pH 7.2). After 4 min incubation at room temperature, optical density at 510 nm was measured with a Unico 2100 visible spectrophotometer (Shanghai, China). A standard curve was generated with known concentrations of chemical H_2O_2.

Quantitative PCR

Total RNA was extracted from the mid-log-phase (OD_{600}, ~0.4 to 0.5) cultures of tested strains using TRIzol reagent (Invitrogen) as recommended by the suppliers. After quality confirmation on 1% agarose gel, RNA extracts were treated with RNase-free DNase (Promega). cDNAs were generated from 2 μg of total RNA with random primers using Moloney Murine Leukemia Virus Reverse Transcriptase (Promega) according to the supplier's instructions and used for qPCR amplification with the corresponding primers (Table S1). Amplifications were performed with a Mastercycler ep realplex2 (Eppendorf AG, Hamburg, Germany). To estimate copy numbers of the *So-aqpA* mRNA, a standard curve of the *So-aqpA* gene was generated by quantitative PCR using 10-fold serially diluted PCR product as the template. The 16S rRNA gene was used as the biomass reference. The number of copies of *So-aqpA* transcript per 1000 16S rRNA copies is shown. All the measurements were done for triplicate samples and repeated at least three times.

Northern blotting

Total RNA was run on 5% Urea-PAGE for 100 min at 250 volts on ice. RNAs in the gel were transferred to positively charged nylon membranes (GE Healthcare) and cross-linked by using GS Gene Linker™ UV Chamber. The membranes were pre-hybridized in buffer (5 × SSC, 5 × Denhardt's, 50% (v/v) deionized formamide, 0.5% (m/v) SDS, and 200 μg/ml salmon sperm DNA) for 4 h, and then hybridized with biotin-labeled NoraqpA (Table S1) at 42 °C overnight. The *So-aqpA* transcript was then detected using Chemiluminescent Nucleic Acid Detection Module Kit (Thermo Fisher Scientific).

Construction of So-aqpA luciferase reporter strain and assay of luciferase activity

The *So-aqpA* luciferase reporter was constructed by inserting the promoter fragment of *So-aqpA* gene into the compatible sites on plasmid pFW5-*luc* (30) which carries luciferase reporter gene. The recombinant plasmid pFW5-P*aqpA-luc* was then transformed into the WT strain to produce P*aqpA-luc* strain. For luciferase activity assay, 100 μl of P*aqpA-luc* cells were collected into 1.5 ml-Eppendorf tubes, exposed to air for 5 min at room temperature, and 25 μl of 1 mM D-luciferin (Sigma-Aldrich) solution (in 1 mM citrate buffer, pH 6.0) was added, and then the assay was performed with a TD 20/20 luminometer (Turner Biosystems, Sunnyvale, CA). The optical density of the samples (OD_{600}) was measured using a 2100 visible spectrophotometer (Unico, Shanghai, China) and used to normalize the luciferase activity. All the measurements were done on triplicate samples and repeated at least three times.

EMSA

The So-*aqpA* promoter fragment was PCR amplified using a biotin-labeled primer pair of aqpAEMSAF/aqpAEMSAR (Table S1). EMSA was performed using Light Shift Chemiluminescent EMSA Kit (Pierce). Briefly, 0.1 nM biotin-labeled dsDNA probe was mixed with various amounts of MntR protein (0–200 nM) in the binding buffer (10 mM Tris-HCl, pH 8.0, 5% glycerol, 50 mM NaCl, 10 μg/ml BSA, 2 ng/μl poly (dI-dC) and 0.1 mM $MnCl_2$). The reaction mixtures stayed at 30 °C for 30 min, and then were electrophoresed on 8% polyacrylamide gel on ice. The DNA-protein complex was transferred onto a nylon membrane and detected by Chemiluminescent Nucleic Acid Detection Module kit (Thermo Scientific).

Heterologous expression in Saccharomyces cerevisiae and observation of GFP fluorescence

The *S. oligofermentans So-aqpA* gene was PCR amplified or fused to the green fluorescence protein (sfGFP) gene. Purified PCR products were double digested by HindIII and BamHI, and then integrated into the compatible sites of the pYES2 yeast expression vector (Thermo Fisher). Correct recombinant pYES2-*So-aqpA*, pYES2-*So-aqpA-gfp*, and pYES2 were transformed into *S. cerevisiae* INVSc1 using a yeast transformation kit (Labest Company, Beijing, China) and selected on SC-Ura medium (Coolaber Company, Beijing, China). Correct transformants were verified by plasmid extraction, PCR, and sequencing.

S. cerevisiae strains carrying *pYES2-So aqpA-gfp* or pYES2 were grown in SC-Ura galactose medium to induce the *So-aqpA-gfp* gene expression. Then 500 μl cells were pelleted, washed with distilled water twice, and resuspended in 100 μl of distilled water in a 1.5 ml Eppendorf tube. After 30-min exposure to air in the dark at room temperature, 40 μl of cells were placed on a glass slide (25 × 75 mm, 1- to 1.2-mm thick), covered with a coverslip (14 × 14 mm, 0.17-mm thick), and then visualized under a confocal laser scanning microscope (Leica TCS SP8, Leica Microsystems, Buffalo Grove, IL). Excitation was provided at 488 nm, and emission was collected from a range of 500 to 600 nm.

Hydrogen peroxide sensitivity assay of S. cerevisiae

Overnight cultures of *S. cerevisiae* INVSc1 strains carrying pYES2-*So-aqpA* or empty vector pYES2 grown in SC-Ura glucose were diluted into SC-Ura galactose medium to a final OD_{600} of 0.4, and then induced at 30 °C for 6 h to allow *So-aqpA* gene expression. After induction, the two strains were diluted to OD_{600} of 0.01, and 10 μl of the dilutions were spotted onto SC-Ura galactose agar plates containing various concentrations of H_2O_2. For minimal inhibitory concentration assay, 100-μl

dilutions were added into a 96-well cell culture plate (Nunc), and 100 μl of 24 mM H_2O_2 were added to the first well and mixed, then 100 μl were taken out and added into the second well. Therefore, 2-fold serially diluted H_2O_2 concentration until 0.09 mM was generated. Growth was recorded after 6 days at 30 °C.

Assay of So-AqpA promoting Escherichia coli to uptake H_2O_2

Overnight cultures of *E. coli* carrying recombinant pIB166-*aqpA* or vacant vector pIB166 were 1:100 diluted into fresh LB and grown at 37 °C. After OD_{600} reached ~0.60, cells were collected by centrifugation at 5000 rpm for 10 min and washed twice with PBS. Cells were then diluted to OD_{600} 0.1 with 10 ml of PBS, and H_2O_2 was added to a final concentration of 150 μM. 750 μl of cell suspension were centrifuged at 12,000 rpm for 2 min at indicated time points, and the residual H_2O_2 content in the supernatant was determined.

Statistical analysis

One-way ANOVA followed by Tukey's post hoc test or Student's *t* test was performed by using PASW Statistics 18 or Excel, respectively. The level of significance was determined at $p < 0.05$.

Author contributions—H. T., F. B., and X. D. conceptualization; H. T. and X. D. formal analysis; H. T. funding acquisition; H. T., X. W., Y. D., Q. H., Z. Z., Y. Z., and L. D. investigation; H. T. methodology; H. T., X. W., Y. D., Q. H., Z. Z., Y. Z., F. B., and X. D. writing-original draft; H. T., F. B., and X. D. writing-review and editing; X. W., Y. D., and Q. H. data curation; X. D. supervision; X. D. project administration.

Acknowledgments—We thank Dr. Jiangyun Wang at the Institute of Biophysics, Chinese Academy of Sciences for providing pHyPer-N1 plasmid; Dr. Yu Fu at Institute of Microbiology, CAS for providing S. cerevisiae; and Dr. Xiaolan Zhang at the Institute of Microbiology, CAS for help in confocal laser scanning microscopy imaging.

References

1. Preston, G. M., Carroll, T. P., Guggino, W. B., and Agre, P. (1992) Appearance of water channels in *Xenopus* oocytes expressing red cell CHIP28 protein. *Science* **256,** 385–387 CrossRef Medline
2. Borgnia, M. J., and Agre, P. (2001) Reconstitution and functional comparison of purified GlpF and AqpZ, the glycerol and water channels from *Escherichia coli. Proc. Natl. Acad. Sci. U.S.A.* **98,** 2888–2893 CrossRef Medline
3. Agre, P., Bonhivers, M., and Borgnia, M. J. (1998) The aquaporins, blueprints for cellular plumbing systems. *J. Biol. Chem.* **273,** 14659–14662 CrossRef Medline
4. Calamita, G., Perret, J., and Delporte, C. (2018) Aquaglyceroporins: Drug targets for metabolic diseases? *Front. Physiol.* **9,** 851 CrossRef Medline
5. Siefritz, F., Tyree, M. T., Lovisolo, C., Schubert, A., and Kaldenhoff, R. (2002) PIP1 plasma membrane aquaporins in tobacco: From cellular effects to function in plants. *Plant Cell* **14,** 869–876 CrossRef Medline
6. Rodrigues, O., Reshetnyak, G., Grondin, A., Saijo, Y., Leonhardt, N., Maurel, C., and Verdoucq, L. (2017) Aquaporins facilitate hydrogen peroxide entry into guard cells to mediate ABA- and pathogen-triggered stomatal closure. *Proc. Natl. Acad. Sci. U.S.A.* **114,** 9200–9205 CrossRef Medline
7. Zardoya, R. (2005) Phylogeny and evolution of the major intrinsic protein family. *Biol. Cell* **97,** 397–414 CrossRef Medline
8. Savage, D. F., O'Connell J. D., 3rd, Miercke, L. J., Finer-Moore, J., and Stroud, R. M. (2010) Structural context shapes the aquaporin selectivity filter. *Proc. Natl. Acad. Sci. U.S.A.* **107,** 17164–17169 CrossRef Medline
9. Törnroth-Horsefield, S., Hedfalk, K., Fischer, G., Lindkvist-Petersson, K., and Neutze, R. (2010) Structural insights into eukaryotic aquaporin regulation. *FEBS Lett.* **584,** 2580–2588 CrossRef Medline
10. Rodrigues, C., Mósca, A. F., Martins, A. P., Nobre, T., Prista, C., Antunes, F., Cipak Gasparovic, A., and Soveral, G. (2016) Rat aquaporin-5 is pH-gated induced by phosphorylation and is implicated in oxidative stress. *Int. J. Mol. Sci.* **17,** E2090 CrossRef Medline
11. Verdoucq, L., Grondin, A., and Maurel, C. (2008) Structure-function analysis of plant aquaporin AtPIP2;1 gating by divalent cations and protons. *Biochem. J.* **415,** 409–416 CrossRef Medline
12. Mósca, A. F., de Almeida, A., Wragg, D., Martins, A. P., Sabir, F., Leoni, S., Moura, T. F., Prista, C., Casini, A., and Soveral, G. (2018) Molecular basis of aquaporin-7 permeability regulation by pH. *Cells* **7,** E207 CrossRef Medline
13. Dynowski, M., Schaaf, G., Loque, D., Moran, O., and Ludewig, U. (2008) Plant plasma membrane water channels conduct the signalling molecule H_2O_2. *Biochem. J.* **414,** 53–61 CrossRef Medline
14. Bienert, G. P., and Chaumont, F. (2014) Aquaporin-facilitated transmembrane diffusion of hydrogen peroxide. *Biochim. Biophys. Acta* **1840,** 1596–1604 CrossRef Medline
15. Al Ghouleh, I., Frazziano, G., Rodriguez, A. I., Csányi, G., Maniar, S., St. Croix, C. M., Kelley, E. E., Egaña, L. A., Song, G. J., Bisello, A., Lee, Y. J., and Pagano, P. J. (2013) Aquaporin 1, Nox1, and Ask1 mediate oxidant-induced smooth muscle cell hypertrophy. *Cardiovasc. Res.* **97,** 134–142 CrossRef Medline
16. Medraño-Fernandez, I., Bestetti, S., Bertolotti, M., Bienert, G. P., Bottino, C., Laforenza, U., Rubartelli, A., and Sitia, R. (2016) Stress regulates aquaporin-8 permeability to impact cell growth and survival. *Antioxid. Redox Signal.* **24,** 1031–1044 CrossRef Medline
17. Miller, E. W., Dickinson, B. C., and Chang, C. J. (2010) Aquaporin-3 mediates hydrogen peroxide uptake to regulate downstream intracellular signaling. *Proc. Natl. Acad. Sci. U.S.A.* **107,** 15681–15686 CrossRef Medline
18. Marinho, H. S., Real, C., Cyrne, L., Soares, H., and Antunes, F. (2014) Hydrogen peroxide sensing, signaling and regulation of transcription factors. *Redox Biol.* **2,** 535–562 CrossRef Medline
19. Rhee, S. G. (2006) H_2O_2, a necessary evil for cell signaling. *Science* **312,** 1882–1883 CrossRef Medline
20. Calamita, G. (2000) The *Escherichia coli* aquaporin-Z water channel. *Mol. Microbiol.* **37,** 254–262 CrossRef Medline
21. Bienert, G. P., Desguin, B., Chaumont, F., and Hols, P. (2013) Channel-mediated lactic acid transport: A novel function for aquaglyceroporins in bacteria. *Biochem. J.* **454,** 559–570 CrossRef Medline
22. Seaver, L. C., and Imlay, J. A. (2001) Hydrogen peroxide fluxes and compartmentalization inside growing *Escherichia coli. J. Bacteriol.* **183,** 7182–7189 CrossRef Medline
23. Tong, H., Chen, W., Merritt, J., Qi, F., Shi, W., and Dong, X. (2007) *Streptococcus oligofermentans* inhibits *Streptococcus mutans* through conversion of lactic acid into inhibitory H_2O_2: A possible counteroffensive strategy for interspecies competition. *Mol. Microbiol.* **63,** 872–880 CrossRef Medline
24. Biswas, I., Jha, J. K., and Fromm, N. (2008) Shuttle expression plasmids for genetic studies in *Streptococcus mutans. Microbiology* **154,** 2275–2282 CrossRef Medline
25. Belousov, V. V., Fradkov, A. F., Lukyanov, K. A., Staroverov, D. B., Shakhbazov, K. S., Terskikh, A. V., and Lukyanov, S. (2006) Genetically encoded fluorescent indicator for intracellular hydrogen peroxide. *Nat. Methods* **3,** 281–286 CrossRef Medline
26. LeBlanc, D. J., Lee, L. N., and Abu-Al-Jaibat, A. (1992) Molecular, genetic, and functional analysis of the basic replicon of pVA380–1, a plasmid of oral streptococcal origin. *Plasmid* **28,** 130–145 CrossRef Medline
27. Lim, J. B., Barker, K. A., Huang, B. K., and Sikes, H. D. (2014) In-depth characterization of the fluorescent signal of HyPer, a probe for hydrogen peroxide, in bacteria exposed to external oxidative stress. *J. Microbiol. Methods* **106,** 33–39 CrossRef Medline

28. Liu, L., Tong, H., and Dong, X. (2012) Function of the pyruvate oxidase-lactate oxidase cascade in interspecies competition between *Streptococcus oligofermentans* and *Streptococcus mutans*. *Appl. Environ. Microbiol.* **78,** 2120–2127 CrossRef Medline
29. Savage, D. F., and Stroud, R. M. (2007) Structural basis of aquaporin inhibition by mercury. *J. Mol. Biol.* **368,** 607–617 CrossRef Medline
30. Podbielski, A., Spellerberg, B., Woischnik, M., Pohl, B., and Lütticken, R. (1996) Novel series of plasmid vectors for gene inactivation and expression analysis in group A streptococci (GAS). *Gene* **177,** 137–147 CrossRef Medline
31. Betzig, E., Patterson, G. H., Sougrat, R., Lindwasser, O. W., Olenych, S., Bonifacino, J. S., Davidson, M. W., Lippincott-Schwartz, J., and Hess, H. F. (2006) Imaging intracellular fluorescent proteins at nanometer resolution. *Science* **313,** 1642–1645 CrossRef Medline
32. Wang, S., Moffitt, J. R., Dempsey, G. T., Xie, X. S., and Zhuang, X. (2014) Characterization and development of photoactivatable fluorescent proteins for single-molecule-based superresolution imaging. *Proc. Natl. Acad. Sci. U.S.A.* **111,** 8452–8457 CrossRef Medline
33. Huang, B., Wang, W., Bates, M., and Zhuang, X. (2008) Three-dimensional super-resolution imaging by stochastic optical reconstruction microscopy. *Science* **319,** 810–813 CrossRef Medline
34. Chen, Z., Wang, X., Yang, F., Hu, Q., Tong, H., and Dong, X. (2017) Molecular insights into hydrogen peroxide-sensing mechanism of the metalloregulator MntR in controlling bacterial resistance to oxidative stresses. *J. Biol. Chem.* **292,** 5519–5531 CrossRef Medline
35. Wang, X., Tong, H., and Dong, X. (2014) PerR-regulated manganese ion uptake contributes to oxidative stress defense in an oral streptococcus. *Appl. Environ. Microbiol.* **80,** 2351–2359 CrossRef Medline
36. Henzler, T., and Steudle, E. (2000) Transport and metabolic degradation of hydrogen peroxide in Chara corallina: Model calculations and measurements with the pressure probe suggest transport of H_2O_2 across water channels. *J. Exp. Bot.* **51,** 2053–2066 CrossRef Medline
37. Imlay, J. A. (2013) The molecular mechanisms and physiological consequences of oxidative stress: Lessons from a model bacterium. *Nat. Rev. Microbiol.* **11,** 443–454 CrossRef Medline
38. Faulkner, M. J., and Helmann, J. D. (2011) Peroxide stress elicits adaptive changes in bacterial metal ion homeostasis. *Antioxid. Redox Signal.* **15,** 175–189 CrossRef Medline
39. Bi, C., Tham, D. K. L., Perronnet, C., Joshi, B., Nabi, I. R., and Moukhles, H. (2017) The oxidative stress-induced increase in the membrane expression of the water-permeable channel aquaporin-4 in astrocytes is regulated by caveolin-1 phosphorylation. *Front. Cell Neurosci.* **11,** 412 CrossRef Medline
40. Beitz, E., Wu, B., Holm, L. M., Schultz, J. E., and Zeuthen, T. (2006) Point mutations in the aromatic/arginine region in aquaporin 1 allow passage of urea, glycerol, ammonia, and protons. *Proc. Natl. Acad. Sci. U.S.A.* **103,** 269–274 CrossRef Medline
41. Bienert, G. P., Møller, A. L., Kristiansen, K. A., Schulz, A., Møller, I. M., Schjoerring, J. K., and Jahn, T. P. (2007) Specific aquaporins facilitate the diffusion of hydrogen peroxide across membranes. *J. Biol. Chem.* **282,** 1183–1192 CrossRef Medline
42. Almasalmeh, A., Krenc, D., Wu, B., and Beitz, E. (2014) Structural determinants of the hydrogen peroxide permeability of aquaporins. *FEBS J.* **281,** 647–656 CrossRef Medline
43. Calamita, G., Kempf, B., Bonhivers, M., Bishai, W. R., Bremer, E., and Agre, P. (1998) Regulation of the *Escherichia coli* water channel gene aqpZ. *Proc. Natl. Acad. Sci. U.S.A.* **95,** 3627–3631 CrossRef Medline
44. Borgnia, M. J., Kozono, D., Calamita, G., Maloney, P. C., and Agre, P. (1999) Functional reconstitution and characterization of AqpZ, the *E. coli* water channel protein. *J. Mol. Biol.* **291,** 1169–1179 CrossRef Medline
45. Bienert, G. P., Bienert, M. D., Jahn, T. P., Boutry, M., and Chaumont, F. (2011) *Solanaceae* XIPs are plasma membrane aquaporins that facilitate the transport of many uncharged substrates. *Plant J.* **66,** 306–317 CrossRef Medline
46. Zhang, Y., Cui, Y., and Chen, L. Y. (2012) Mercury inhibits the L170C mutant of aquaporin Z by making waters clog the water channel. *Biophys. Chem.* **160,** 69–74 CrossRef Medline
47. Tong, H., Gao, X., and Dong, X. (2003) *Streptococcus oligofermentans* sp. nov., a novel oral isolate from caries-free humans. *Int. J. Syst. Evol. Microbiol.* **53,** 1101–1104 CrossRef Medline
48. Lau, P. C., Sung, C. K., Lee, J. H., Morrison, D. A., and Cvitkovitch, D. G. (2002) PCR ligation mutagenesis in transformable streptococci: Application and efficiency. *J. Microbiol. Methods* **49,** 193–205 CrossRef Medline
49. Liu, Y., Zeng, L., and Burne, R. A. (2009) AguR is required for induction of the *Streptococcus mutans* agmatine deiminase system by low pH and agmatine. *Appl. Environ. Microbiol.* **75,** 2629–2637 CrossRef Medline